

Evaluation of surface displacement equation due to tunnelling in cohesionless soil

Sherif A. Mazek *

Civil Engineering Department, Military Technical College, Kobbry El-Kobba, Khelifa El-Maamoon, Cairo, Egypt

(Received January 10, 2014, Revised February 27, 2014, Accepted March 06, 2014)

Abstract. The theoretical predictions of ground movements induced by tunnelling are usually based on the assumptions that the subsoil has the same soil densities. The theoretical prediction does not consider the impact of different sand soil types on the surface settlement due to tunnelling. The finite elements analysis (FEA) considers stress and strength parameters of the different sand soil densities. The tunnel construction requires the solution of large soil–structure interaction problem. In the present study, the FEA is used to model soil-tunnel system performance based on a case study to discuss surface displacement due to tunnelling. The Greater Cairo metro tunnel (Line 3) is considered in the present study as case study. The surface displacements obtained by surface displacement equation (SDE) proposed by Peck and Schmidt (1969) are presented and discussed. The main objective of this study is to capture the limitations of the parameters used in the SDE based on the FEA at different sand soil densities. The study focuses on the parameters used in the SDE based on different sand soil densities. The surface displacements obtained by the FEA are compared with those obtained by the SDE. The results discussed in this paper show that the different sand soil densities neglected in the SDE have a significant influence on the surface displacement due to tunnelling.

Keywords: tunnels; surface settlement; surface displacement equation; deformations

1. Introduction

Tunnels solve many problems such as waste water, power supplies, and traffic jam (Mazek and El-Tehawy 2008). Several tunnels have been constructed worldwide to solve the transportation problems such as the Greater Cairo Metro and El-Azhar road tunnels (El-Nahhass 1999, NAT 1993, 1999, 2010). These tunnels are considered as major projects in Cairo city. There are technologies to assist in excavation such as tunnelling boring machine (TBM) and cut and cover method (Bicel and Kuesel 1982).

It is necessary to investigate the geotechnical problems related to tunnelling for better understanding the performance of the tunnel system. Many geotechnical problems were encountered during the construction of the Greater Cairo metro, El-Azhar road tunnels, and the Greater Cairo sewage tunnel. Most problems are related to the damage of surrounding buildings due to surface and subsurface ground subsidence (Abu-Krishna 2001). Tunnelling in cohesionless

*Corresponding author, Professor, E-mail: samazek@yahoo.com

soil is a sophisticated process leading to move surface and subsurface structures (Mazek and El-Tehawy 2008, Mroueh and Shahrouh 2008). Ground movement is caused by tunnelling through soft ground due to the associated stress change due to tunnel advancing.

Wang *et al.* (2011) applied finite element analysis to investigate the effect of tunnelling induced ground movement on buried pipelines. Zhang *et al.* (2011) discussed the theoretical predictions of ground movements induced by tunnelling. The theoretical predictions were based on the assumptions that the ground was homogenous. Layered formations with different soil properties were usually encountered in situ and effects of soil stratification should be taken into account. They showed that the soil stratification, neglected in previous solutions, had a significant influence on the tunnelling-induced ground movements in multi-layered soils. Elsayed (2011) used 2-D finite element analysis (FEA) to model two phases of tunnelling process. First phase, the excavation phase was responsible to determine the pre-lining rock mass deformations and the reduced in-situ stresses. Second phase, the interaction phase modeled the compatibility of the rock-lining system. The deformations and stresses of the rock-lining system and the final rock mass pressure acting on the lining were determined. Cavalaro *et al.* (2011) analyzed the influence of the contact deficiencies between the segmented tunnel lining during the construction of tunnels and the consequent damage procedure with TBM. They used the finite element analysis to simulate the contact deficiencies.

Darabi *et al.* (2012) presented an appropriate model to predict the behavior of the tunnel in Tehran No. 3 subway line. They employed empirical methods to determine the variation of radial displacements along the longitudinal direction of a tunnel. They also determined the tunnel deformation using numerical analyses. Valizadeh Kivi *et al.* (2012) investigated settlement control of large span underground station in Tehran metro using 3-D finite element analysis. They discussed the impact of central beam column (CBC) on the rigidity of the supporting tunnel system. Liu *et al.* (2012) discussed the ground movement property caused by shield tunnelling and expanding construction. Ground movement and construction influence were obtained by numerical model. Wang *et al.* (2012) used finite element analysis to predict surface settlement above tunnel in clay till. The influence of drainage condition on surface settlement was investigated.

Jongpradist *et al.* (2013) used three-dimensional elasto-plastic numerical analysis to investigate the influences of tunnel excavation on existing loaded piles. The effects of parameter on pile responses to be used as criteria for suggesting the influence zones were captured from the analysis method. Garner and Coffman (2013) proposed a numerical method based on an acceptable ground surface settlement profile to generate a tunnel system configuration that reproduced the acceptable settlement profile. They presented a brief discussion of existing methods of tunnel settlement analysis and two case studies illustrating the proposed method. Each case study was used to illustrate the use of bifurcated static back calculation – iterative from the finite element model prediction method.

The numerical techniques are widely used to predict the ground movements. During the last three decades, numerical analysis has been grown rapidly (Abu Krisha 2001, El-Nahhass 1986, 1999, Mazek 2005). Finite element method is considered the most appropriate analytical technique to solve geotechnical problems (Abu-Farsakh and Tumay 1999, Mazek *et al.* 2004, Vermeer and Moller 2008). Modeling of geotechnical properties and details of tunnelling procedure are the sophisticated geotechnical problem (Chehade and Shahrouh 2008, El-Nahhass 1986, Mazek 2004, 2005, Oettl *et al.* 1998).

The surface displacement is calculated by both the FEA and the SDE developed by Peck and Schmidt (1969) based on different sand soil densities. The SDE does not consider the impact of

different sand soil densities on the surface displacement. An extensive study is also conducted to discuss the impact of different tunnel diameters (D), different ground losses (V_L), and different tunnel depths (Z) on surface settlement due to tunnelling. The parameters used in the SDE are discussed and captured based on the FEA to predict surface displacement.

2. Finite element model

The finite element computer program (COSMOS/M) is used in the present study. The finite element model (FEM) takes into account the effects of the vertical overburden pressure, the lateral earth pressure, the non-linear properties of the soil, and the linear properties of the metro tunnel liner. The soil, the metro tunnel liner, and the interface medium are simulated using appropriate finite elements. Fig. 1 shows the typical cross section of the soil profile along the Greater Cairo metro-Line 3 (after NAT 2010). The numerical modeling of the metro tunnel must reflect the

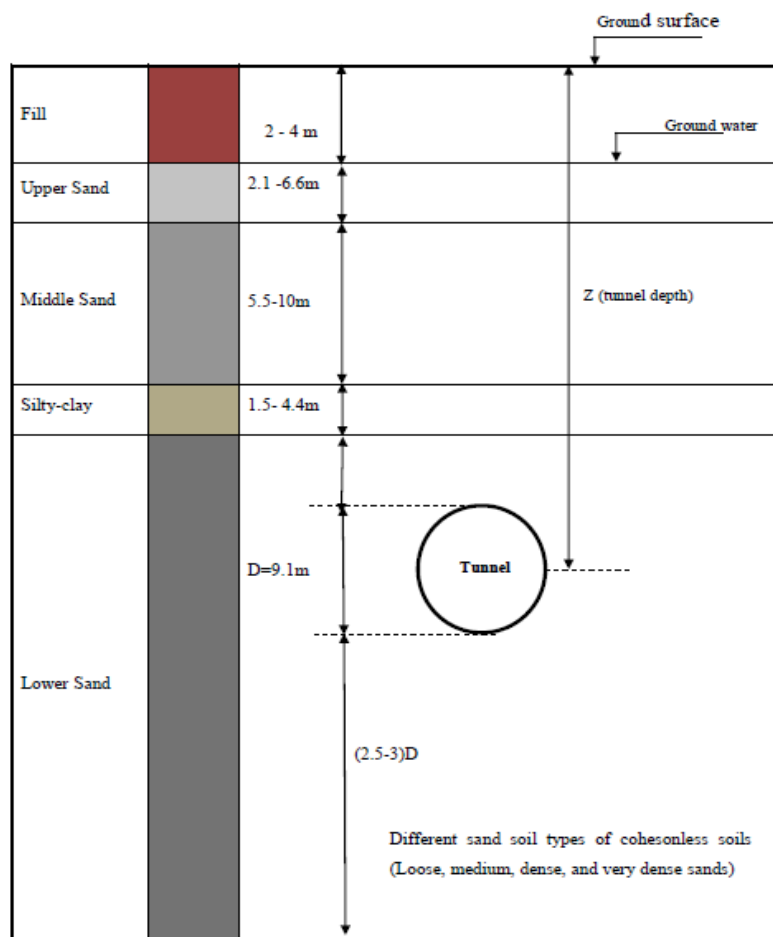


Fig. 1 Typical cross section shows soil profile along the Greater Cairo metro-Line 3 (after NAT 2010)

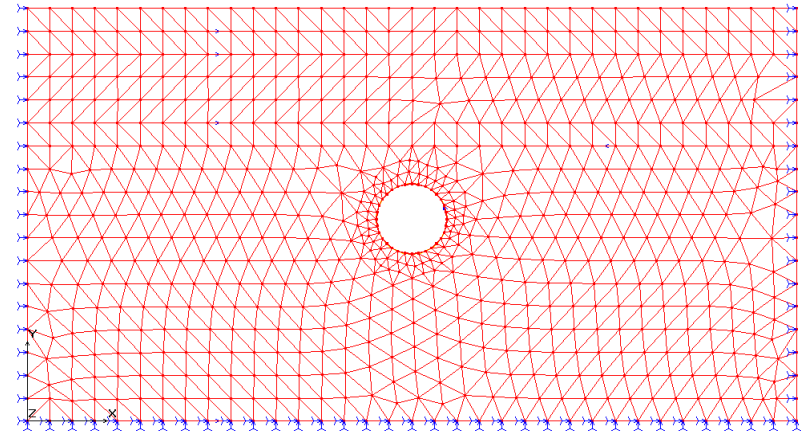


Fig. 2 2-D finite element model of the Greater Cairo Metro-Line 3

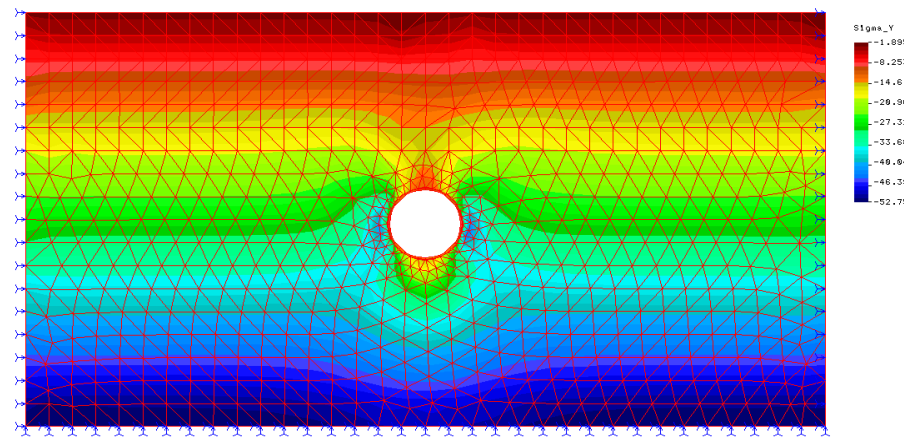


Fig. 3 Calculated final vertical stress around the metro tunnel

characteristic of the ground continuum and the metro tunnel. In addition, the interface between the soil media and the tunnel liner should be idealized in the numerical model.

2-D plane strain elements are used for modeling the soil media and 2-D beam elements for modeling the metro tunnel liner, as shown in Fig. 2. Three-node triangular plane strain elements are adopted to simulate behavior of the soil media. The 2-D beam element and the triangular plane strain element interface is used between the soil media and the tunnel liner to ensure the compatibility conditions at the interface between them as well as the associated stress and strains along the interface surface.

The horizontal plane at the bottom of the mesh is represented by a rigid bedrock layer and the movement at this plane is restrained in all directions. The vertical boundaries of the 2-D FEM are restrained by roller supports to prevent a movement normal to the boundaries. The movement at the upper horizontal plane is free to simulate a free ground surface. The 2-D finite element mesh is shown in Fig. 2.

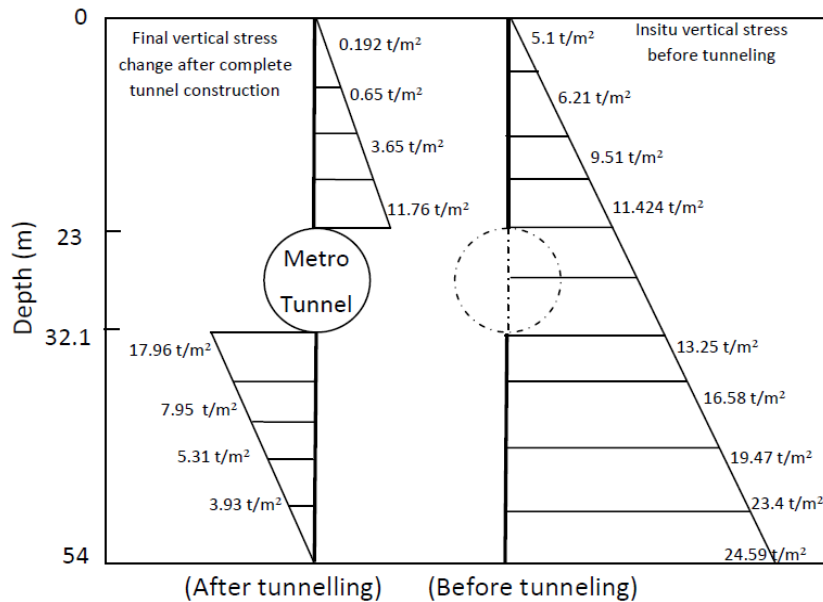


Fig. 4 Vertical stress before and after tunnelling (The Greater Cairo Metro tunnel-Line 3)

The finite element analysis is carried out to simulate the construction of Line 3. The stress changes in surrounding soil due to tunnelling are investigated to study the detailed soil behavior around the metro tunnel. The stresses in the subsoil have undergone three phases of change. At these phases, the loading steps of the metro tunnel construction are simulated using the 2-D FEA.

First phase, the initial principal stresses are computed with the absence of the metro tunnel. Second phase, the excavation of the metro tunnel is modeled by means of the FEM. The excavation is simulated by the removal of those elements inside the boundary of the metro tunnel surface to be exposed by the excavation. The excavated tunnel boundary is free to move until the soil comes into contact with the metro tunnel liner resulting from volume loss. The volume loss is considered in this study. Third phase, the calculated changes in stresses are then added to the initial principal stresses computed from the first phase to determine the final principal stresses resulting from the metro tunnel construction. Fig. 3 shows final vertical stress around the metro tunnel system. The initial in-situ vertical stresses before tunnelling are calculated and plotted in Fig. 4. The final vertical stress change after tunnelling is calculated and shown in the same figure.

3. Boundary condition of tunnel system

A parametric study is conducted to choose the suitable geometric boundaries of the 2-D numerical model. The 2-D numerical model should reflect the behavior of the metro tunnel in the field. The 2-D finite element mesh models soil block width and depth in x and y directions, respectively, as shown in Fig. 2. The calculated surface settlements of the metro tunnel against different model widths are shown in Fig. 5. When the numerical model width exceeds 100 meters there is no change in the estimated surface settlement.

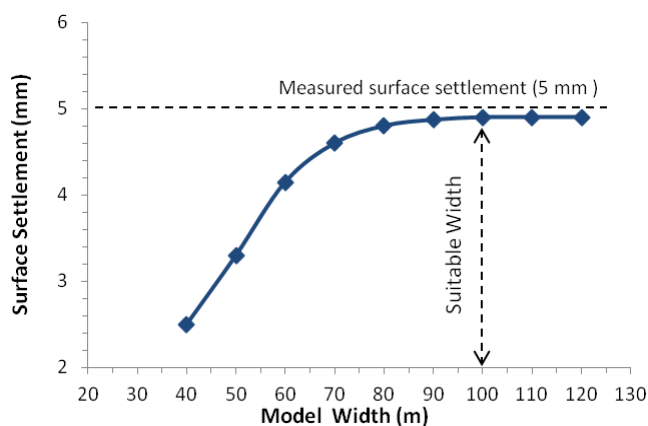


Fig. 5 Calculated surface settlement against different model widths due to tunnelling

Table 1 Estimated surface settlement considering different elements sizes

Mesh size (m)	Element size along outer boundary of soil block mesh		5 m		4 m		3 m*		2 m		1 m
	Element size along tunnel liner		1 m	2m	1 m	2 m	1m*	2 m	1 m	2 m	1 m
	Surface settlement (mm)		4.4	4	4.6	4.15	4.9	4.2	4.9	4.28	4.9

*Selected element size of the 2-D finite element model

The model mesh size is also studied to reflect the performance of the metro tunnel system based on the 2-D FEA. The element size is varied from 2 m, 3 m, 4 m, up to 5 m along the outer boundary of the soil model block. The element size is also varied from 1 m, 1.5 m, 2 m, 2.5 m, up to 3 m along the metro tunnel liner. The calculated surface settlement based on different element sizes is presented in Table 1. The results reveal that as the element size along the outer boundary of the soil model block is smaller than three meters there is no change in calculated surface settlement due to tunnelling. The results also show that as the element size along the metro tunnel liner is smaller than one meter there is no change in calculated surface settlement.

The element size is chosen to be three meters along the outer boundary of the soil block. The element size is chosen to be one meter along the boundary of the tunnel liner because of the high stress change due to tunnel excavation.

The volume loss (V_L) is the ratio of the difference between excavated soil volume and tunnel volume over excavated soil volume. The V_L is studied and varied from 1.5% to 4.5%. Fig. 6 shows the calculated surface settlement along C.L of the metro tunnel at different volume losses.

4. Greater Cairo Metro-Line 3 (Case study)

The Greater Cairo metro tunnel (Line 3) from Attaba station to Abasia station presented and discussed in the present study as a case study. Fig. 7 shows the plan of the Greater Cairo metro-Line 3. 2-D nonlinear numerical model is proposed using the FEA to understand

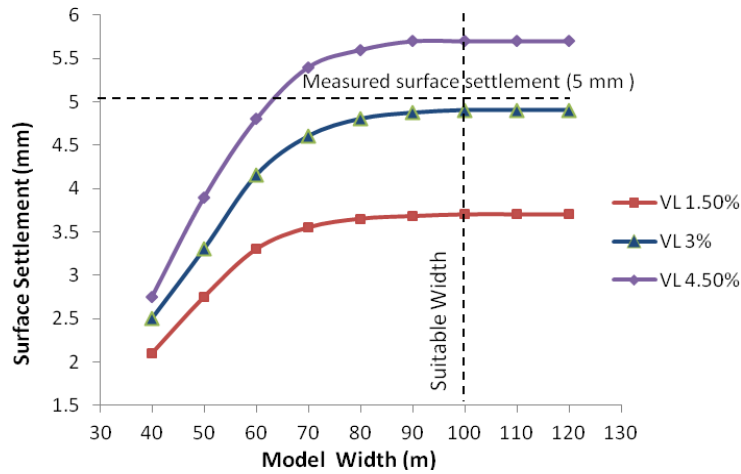


Fig. 6 Calculated surface settlement along C.L of metro tunnel at different volume losses

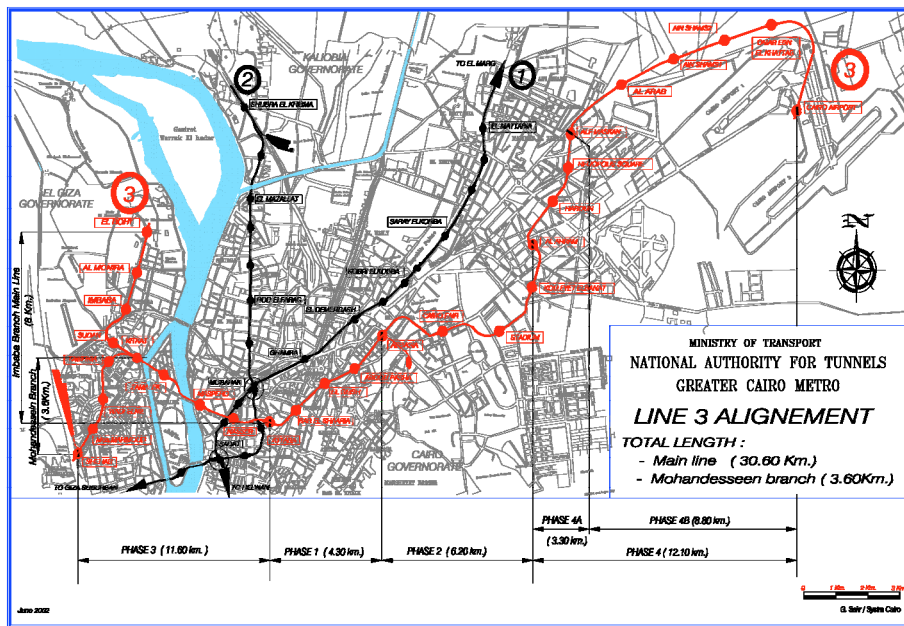


Fig. 7 Plan of the Greater Cairo metro (Line 3) (after NAT 2010)

performance of tunnel system based on a case study. The constitutive model for this analysis utilizes elasto-plastic materials. A yielding function of the Mohr-Coulomb type and a plastic potential function of the Drucker-Prager type are employed (Chen and Mizuno 1990). The nonlinear parameters of different sand soil types are presented in Table 2. A linear constitutive model is employed to represent the tunnel liner. The mechanical properties of metro tunnel liner are tabulated in Table 3.

Table 2 Geotechnical soil parameters

Layer	Fill	Upper sand	Middle sand	Silty-clay	Loose sand	Medium sand	Dense sand (lower layer)	Very dense sand
Bulk density γ_b (t/m ³)	1.7	1.9	1.95	1.8	1.8	1.85	1.9	2.0
Drained poisson's ratio ν_s	0.3	0.3	0.3	0.35	-	-	-	-
Effective angle of initial friction (ϕ)°	27	36	38	29	27	32	38	43
Effective cohesion C (t/m ²)	0	0	0	0	0	0	0	0
Modulus number (m)	300	400	500	325	300	500	800	1000
Exponent number (e)	0.74	0.55	0.52	0.6	0.6	0.51	0.5	0.4
Coefficient of lateral earth pressure K_0	1	0.412	0.385	0.8	0.56	0.47	0.38	0.32
Initial poisson's ratio (G)	-	0.32	0.32	-	0.35	0.32	0.30	0.25
Rate of increase of ν_i with increase in residual strain (d)	-	5	5	-	5	5	5	5
Reduction of ν_i for a 10-fold increase in σ_3 (F)	-	0.17	0.17	-	0.2	0.18	0.16	0.15
R_f	0.69	0.74	0.79	0.7	0.74	0.79	0.85	0.9

Table 3 Mechanical properties of metro tunnel liner

Type	E_b (t/m ²)	(t) cm	F_c (t/m ²)	γ (t/m ³)	V
Tunnel liner	2.1×10^6	50	4000	2.5	0.20

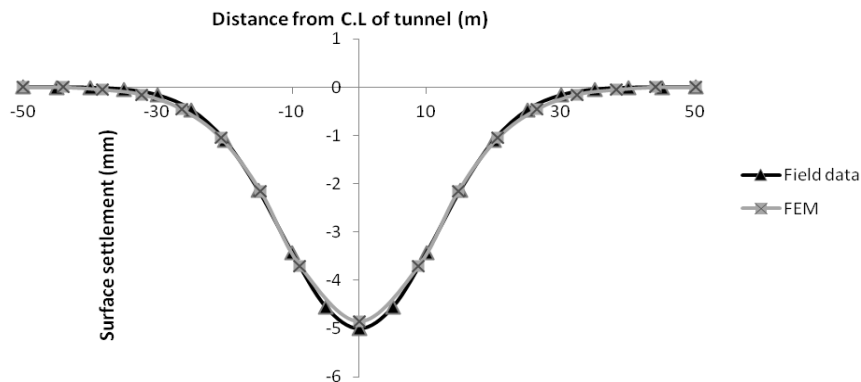


Fig. 8 Comparison between measured and calculated surface settlements along the centreline of the Grater Cairo metro tunnel-Line 3

The 2-D FEA is also adopted to estimate surface settlement and vertical displacement at different locations and levels around tunnel system. The finite element mesh size of the proposed finite element model is studied. Model boundaries and volume losses (V_L) are also discussed to understand the performance of the metro tunnel. Based on this study, the parametric study is

conducted at volume loss of 3%. The associated stress changes in soil due to tunnelling are studied. The results obtained by the 2-D FEA are compared with those obtained by the field reading to assess the accuracy of the proposed 2-D finite element model as shown in Fig. 8. There is a good agreement between the measured readings and the calculated results.

5. Ground response using 2-D finite element analysis

Based on the 2-D FEA, one can proceed to predict ground response due to tunnelling using different sand soil densities. In this study, loose sand, medium sand, dense sand, and very dense sand are considered around tunnel to study surface settlement due to tunnelling. The nonlinear parameters of different sand soil types are presented in Table 2. The numerical analysis is carried out using the drained soil modulus (E_s) calculated by the Janbu equation (Janbu 1963) (Eq. (1)) using different soil parameters as summarized in Table 2 (Duncan *et al.* 1980). The different soil parameters (m , e) are selected to simulate the behaviour of different soil types.

$$E_s = mP_a \left(\frac{\sigma_3}{P_a} \right)^e \quad (1)$$

In which; the modulus number (m) and the exponent number (e) are both pure numbers, σ_3 is the effective confining pressure, and (P_a) is the value of the atmospheric pressure expressed in appropriate units.

The nonlinear properties of soil and the confining pressure (σ_3) are applied in the 2-D FEA to predict the surface displacement due to tunnelling. The tangent modulus (E_t) is also varied with stress level ($\sigma_1 - \sigma_3$), as shown in Eq. (2) (Duncan *et al.* 1980). The nonlinear parameters for the sand soil are presented in Table 2 (NAT 1993, 1999, 2010).

$$E_t = \left[1 - \frac{R_f (1 - \sin \phi) (\sigma_1 - \sigma_3)}{(2c) \cos \phi + 2\sigma_3 \sin \phi} \right]^2 E_s \quad (2)$$

In which; R_f is the failure ratio or the ratio between the compressive strength $(\sigma_1 - \sigma_3)_f$ and the value $(\sigma_1 - \sigma_3)_{ult}$ of the asymptotic stress for the hyperbolic stress-strain curve.

Duncan *et al.* (1980) used the Young's modulus and Poisson's ratio or the bulk modulus to imply the effect of the volume change. The volume change component refers to the variation of volumetric strain (ϵ_v), which varies with the principal strain (ϵ_1). Therefore, Duncan *et al.* (1980) used hyperbolic function to model the stress dependent characteristics of the volumetric strain. The tangent Poisson's ratio implies that the volume change is a hyperbolic function and stress dependent. The parameter (G) is the initial Poisson's ratio (v_i), (F) is the reduction of v_i for a 10-fold increase in σ_3 , and (d) is the rate of increase of v_i with increase in residual strain as presented in Table 2 (NAT 1993, 1999, 2010). The tangent Poisson's ratio (v_t) is computed as presented in Eq. (3) (Wong and Duncan 1974).

$$v_t = \left[\frac{G - F \log \left(\frac{\sigma_3}{P_a} \right)}{\left[1 - d \left(\frac{\sigma_1 - \sigma_3}{E_t} \right) \right]^2} \right] \quad (3)$$

6. Ground response using surface displacement equation

In this study, surface settlement around the centreline of tunnel is calculated by surface displacement equation (SDE) developed by Peck and Schmidt (1969). Peck and Schmidt proposed empirical equation to calculate surface displacement profile due to tunnelling, as presented in Eq. (4).

$$S = S_{\max} \exp\left(\frac{-x^2}{2i^2}\right) \quad (4)$$

In which; S is the surface displacement, S_{\max} is the maximum surface settlement at the point above the tunnel centreline, x is the distance from the tunnel centreline in transverse direction, and i is the horizontal distance from the tunnel axis to the point of inflexion of the settlement trough.

The surface displacement profile could be represented by Gaussian distribution curve as presented in Fig. 9. Attewell *et al.* (1986) proposed (i) parameter adopted in the SDE, as written in Eq. (5).

$$\frac{i}{R} = a \left(\frac{Z_0}{2R}\right)^n \quad a = 0.8 \text{ to } 1.0 \quad n = 0.8 \text{ to } 1.0 \quad (5)$$

Where; Z_0 is the depth of the tunnel springline below ground surface and R is tunnel diameter.

The study also examined the results obtained by the SDE with different (a) and (n) parameters. The (a) parameter is varied from 0.8 to 1 (0.8, 0.9 and 1). The (n) parameter is varied from 0.8 to 1 (0.8, 0.9, and 1).

The maximum surface settlement (S_{\max}) used in the SDE is determined by the 2-D FEA and the field measurements. The surface displacement induced by tunnelling based on different sand soil types are predicted by both the 2-D FEA and the SDE. The FEA and the SDE are also used to calculate surface settlement due to tunnelling based on different tunnel diameters (D), different volume losses (V_L), and different (Z/D) ratios. The surface displacement profiles obtained by the FEA are examined with those obtained by the SDE.

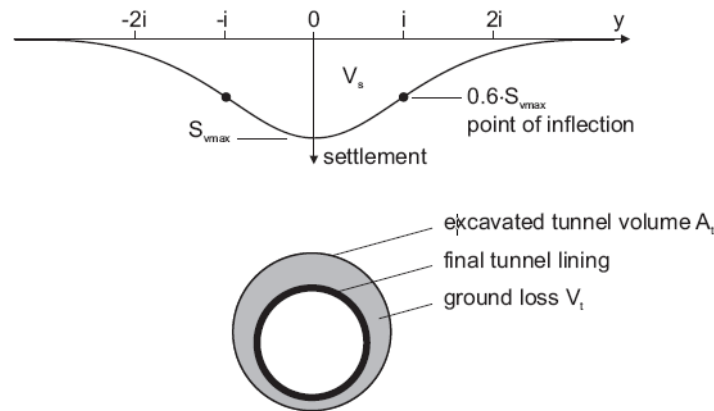


Fig. 9 Gaussian curve for transverse settlement trough (after Peck and Schmidt 1969)

7. Tunnel performance under various parameters

The soil investigation is discussed and analyzed in this study. Five distinct soil layers are encountered. The soil parameters are presented in Table 2. The different types of cohesionless soils are also considered in this study. The different soil parameters (m , e) are selected to simulate the performance of different soil types (Duncan *et al.* 1980).

The tunnel is located at different types of cohesionless soils (loose sand, medium sand, dense sand, and very dense sand). The diameter of the tunnel is varied from 7.5 m, 10 m, 12.5 m and 15 m. The numerical analysis is carried out using the drained soil modulus (E_s) calculated by Janbu equation (1963) as the metro tunnel passes through the sand soil.

8. Surface displacement due to tunnelling

The tunnels constructed in soft ground leads to ground movement (Mroueh and Shahrour 2008). In urban environment, this movement can affect surface and subsurface structures. Prediction of ground movement caused by tunnelling is a major engineering challenge. The FEA and the SDE are used to predict the soil movement by the tunnel excavation in soft ground. In this Section, the results obtained by the SDE are compared with those obtained by FEA.

8.1 Ground response under loose sand impact

Parametric studies are conducted at different tunnel depths from the ground surface. The soil depth underneath tunnel invert is set to be three times the tunnel diameter (Mazek 2005). Fig. 2 shows cross section of tunnel constructed in different sand soils.

Different tunnel diameters (D), different overburden depths (Z), and different volume losses are discussed and presented to predict ground response due to tunnelling. To study ground response under different sand soil types, tunnel diameter is varied from 7.5 m up to 15 m. Z/D ratio is varied from 2.5 to 4. The volume loss (V_L) is also varied from 1.5% to 4.5%.

The surface displacements obtained by the SDE are calculated based on different (a) and (n) parameters. The (a) parameter is varied from 0.8, 0.9, up to 1.0. The (n) parameter is varied from 0.8, 0.9, up to 1.0. The surface settlement profile obtained by both the FEA and the SDE in loose sand is shown in Fig. 10 at V_L of 2.5%, $D = 15$ m, and $Z/D = 3$.

8.2 Ground response under medium sand impact

Surface settlement due to tunnelling is also calculated for the case of medium sand soil. The different soil parameters (m , e) are selected to simulate the behavior of medium sand soil (Duncan *et al.* 1980).

The surface settlement profile is predicted by both the FEA and the SDE. The study also considered different tunnel diameters (D), different volume losses (V_L), and different Z/D ratios. In the parametric study, the V_L is varied from 1.5% to 4.5%. The tunnel diameter is varied from 7.5 m, 10 m, 12.5 m, to 15 m. The Z/D ratio is also varied from 2.5, 3, 3.5, 4, 4.5, to 5.

The surface displacements are computed by the SDE based on different (a) and (n) parameters. The (a) parameter is varied from 0.8, 0.9 up to 1.0. The (n) parameter is varied from 0.8, 0.9 up to 1.0. The Surface settlement profile obtained by both the FEA and the SDE is shown in Fig. 11 based on V_L of 2.5%, $D = 15$ m, and $Z/D = 3$.

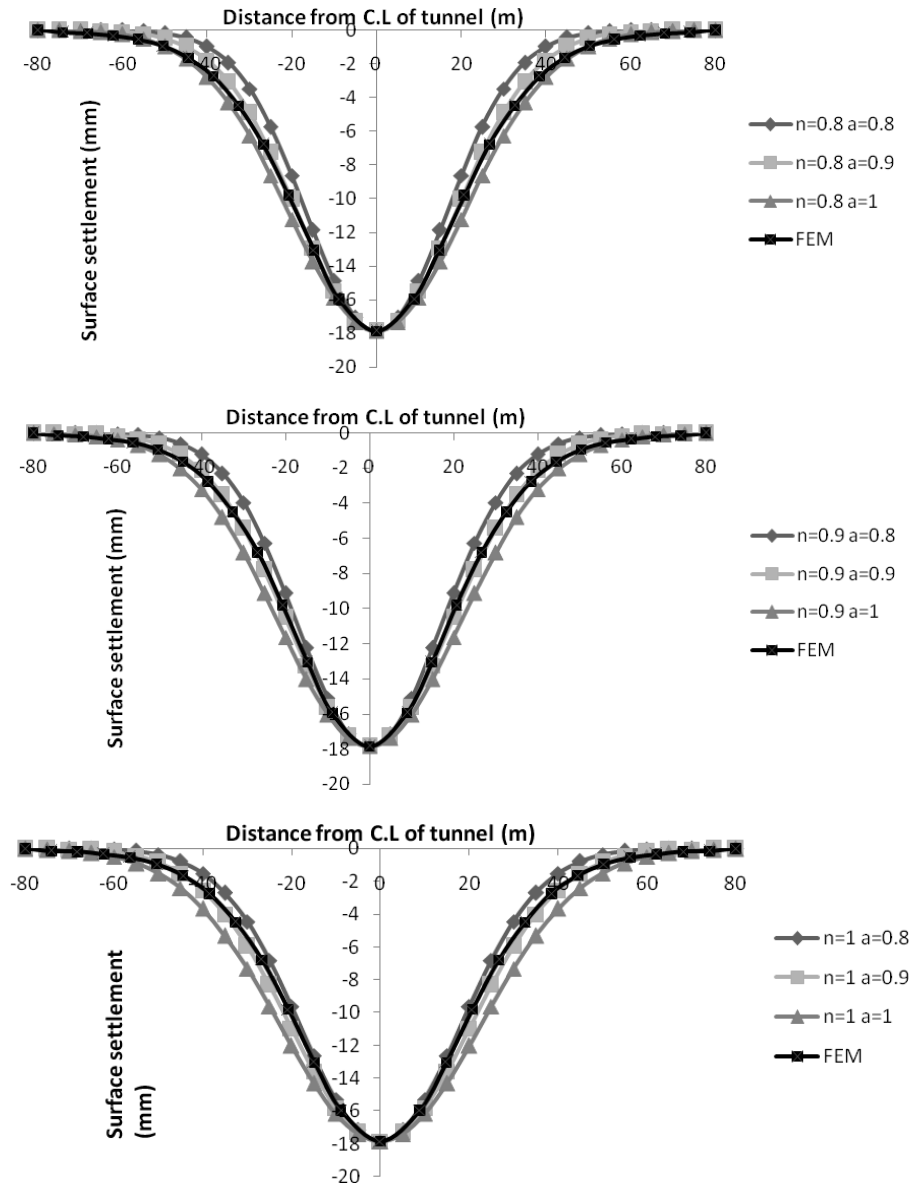


Fig. 10 Surface settlement profile obtained by both finite element analysis and surface displacement equation in loose sand (ground loss of 2.5%, $D = 15$ m, $Z/D = 3$)

8.3 Ground response under dense sand impact

The surface displacement is calculated by both the SDE and the FEA for dense sand due to tunnelling. The surface displacement profile is computed by the FEA and the SDE. The soil parameters (m , e) are selected to simulate the behavior of dense sand as presented in Table 1 (Duncan *et al.* 1980).

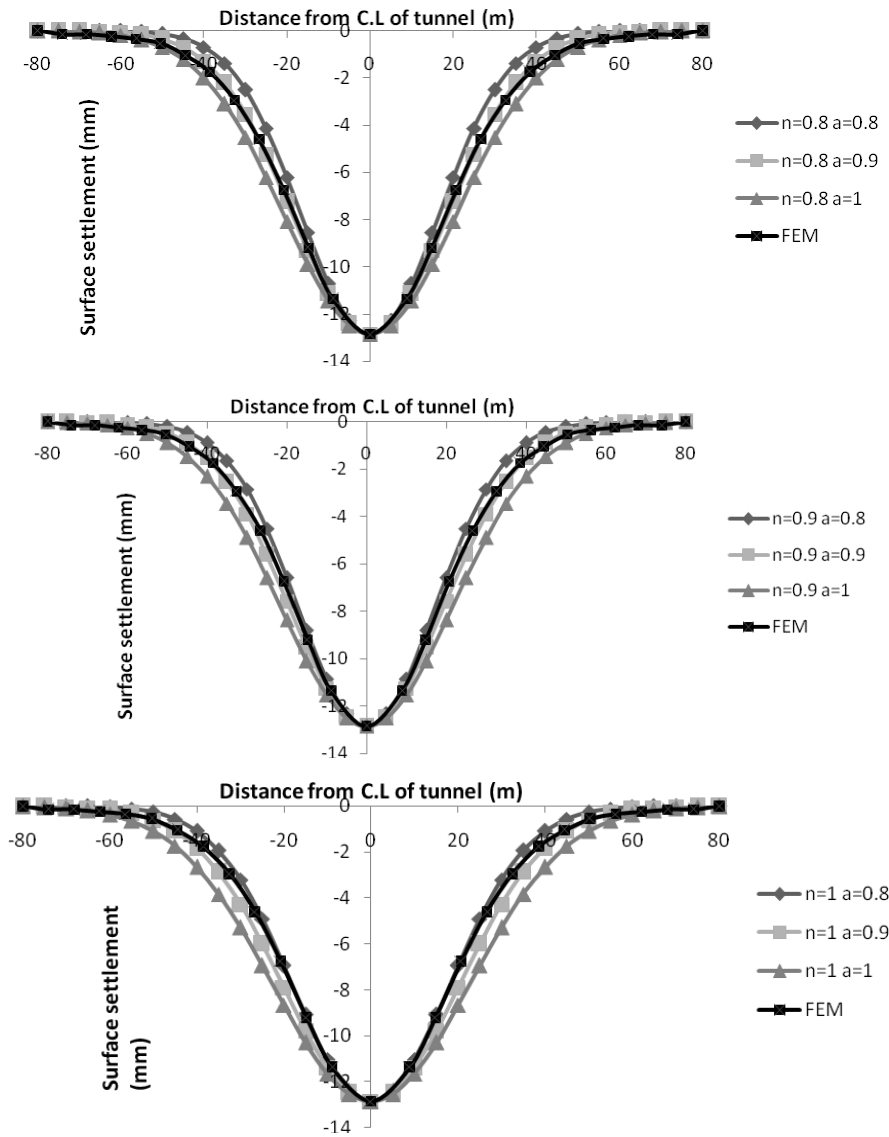


Fig. 11 Surface settlement profile obtained by both finite element analysis and surface displacement equation in medium sand (ground loss of 2.5%, $D = 15$ m, $Z/D = 3$)

The surface settlements are calculated by both the FEA and the SDE based on different tunnel diameters (D), different volume losses (V_L), and different tunnel depths (Z). The volume loss is varied from 1.5% to 4.5%. The tunnel diameter is varied from 7.5 m, 10 m, 12.5 m, to 15 m. The (Z/D) ratio is ranged from 2.5, 3, 3.5, to 4.

The surface displacements are calculated by the SDE based on different (a) and (n) parameters. The (a) parameter is varied from 0.8, 0.9, up to 1.0. The (n) parameter is varied from 0.8, 0.9, up to 1.0. The surface settlement profile obtained by both the FEA and the SDE is shown in Fig. 12 at V_L of 2.5%, $D = 15$ m, and $Z/D = 3$.

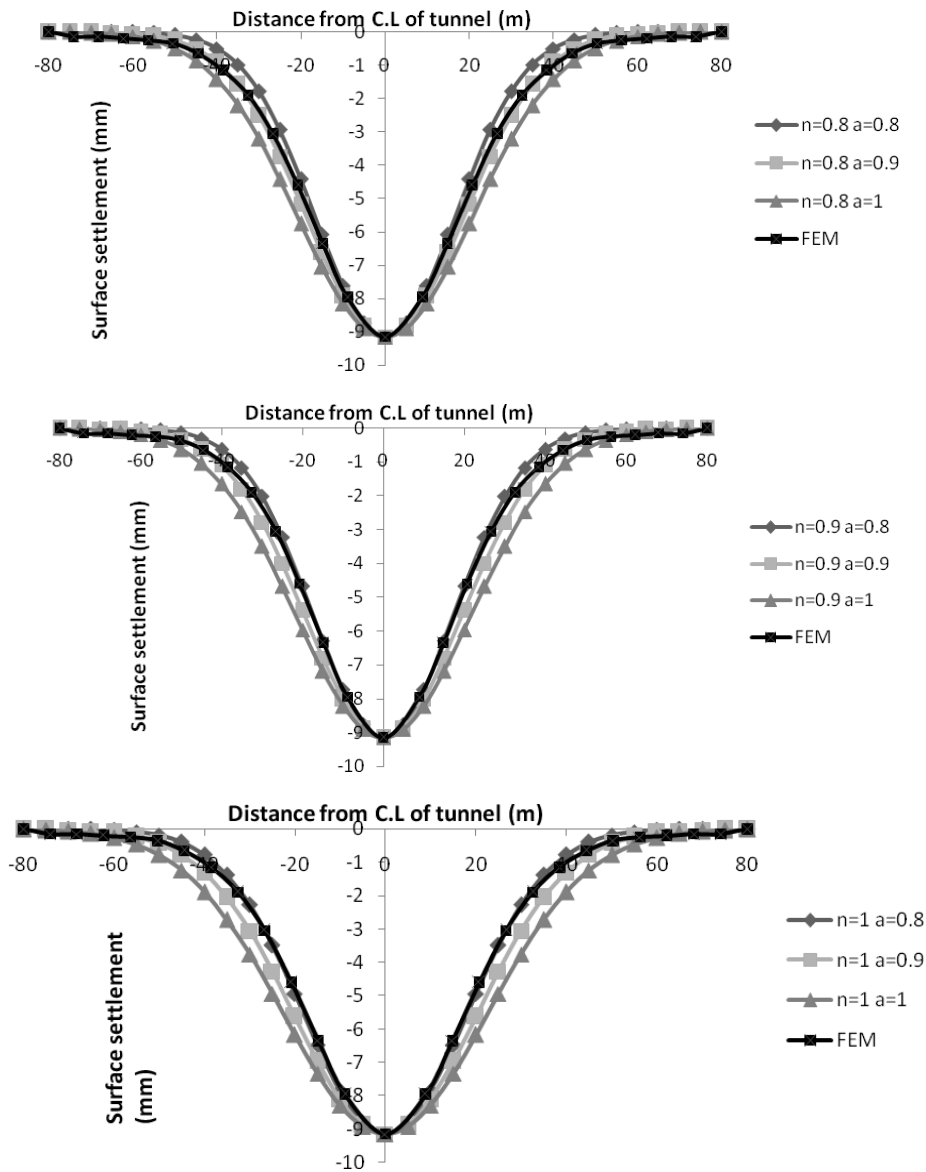


Fig. 12 Surface settlement profile obtained by both finite element analysis and surface displacement equation in dense sand (ground loss of 2.5%, $D = 15$ m, $Z/D = 3$)

8.4 Ground response under very dense sand impact

To further understand the ground response due to tunnelling, the ground surface displacement is calculated by both the SDE and the FEA at the case of very dense sand. The soil parameters (m , e) are selected to simulate the behavior of very dense sand (Duncan *et al.* 1980).

The parametric study also considers different tunnel diameters, different volume losses, and different overburden depths. In the parametric study, the volume loss is varied from 1.5% to 4.5%.

The tunnel diameter is varied from 7.5 m, 10 m, 12.5 m, to 15 m. The Z/D ratios are ranged from 2.5, 3, 3.5, to 4.

The surface displacements are calculated by the SDE based on different (a) and (n) parameters. The (a) parameter is varied from 0.8, 0.9, up to 1.0. The (n) parameter is varied from 0.8, 0.9 up to 1.0. The surface settlement profile obtained by both the FEA and the SDE is shown in Fig. 13 at V_L of 2.5%, $D = 15$ m, and $Z/D = 3$.

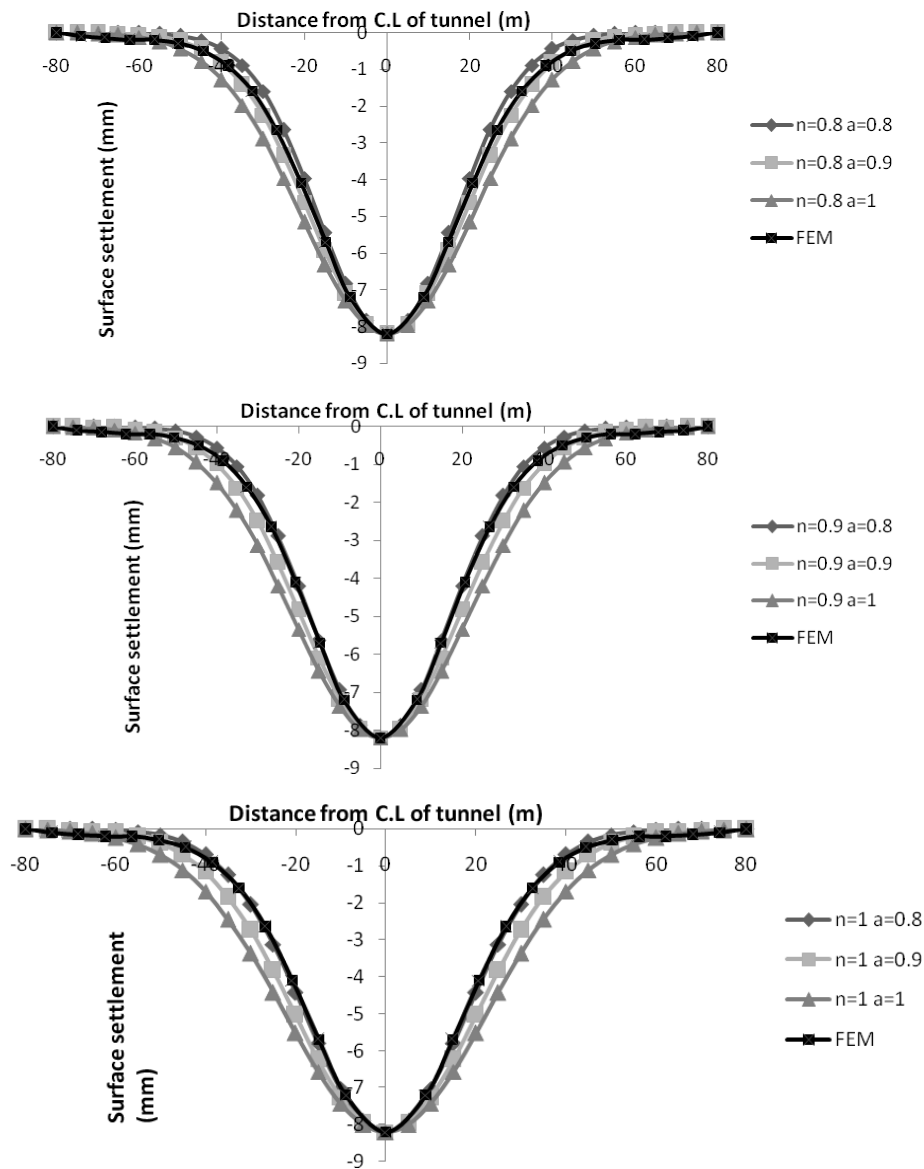


Fig. 13 Surface settlement profile obtained by both finite element analysis and surface displacement equation in very dense sand (ground loss of 2.5%, $D = 15$ m, $Z/D = 3$)

9. Discussions

The surface displacement profile computed by the FEA and the SDE are studied and compared based on different sandy soil densities. The surface settlement due to tunnelling is also calculated by the SDE based on different volume losses, different overburden depths (Z) and different (a) and (n) parameters, as shown in Figs. 10 to 13. The (a) parameter is varied from 0.8, 0.9, up to 1.0. The (n) parameter is varied from 0.8, 0.9, up to 1.0. In this study, the volume loss is considered to be 2.5%. The tunnel diameter is considered to be 15 m. The Z/D ratio is equal to 3. The finite element analysis takes into account strength and stress parameters of different sand soil types. However, the surface displacement equation proposed by Peck and Schmidt (1969) does not consider the impact of different sand densities.

The difference between the two sets of computed settlements is noticed in different sand densities (loose, medium, dense, and very dense). The difference between the two sets of computed settlements lies on the use of the width parameter equation (i), as presented in Fig. 1 (Attewell *et al.* 1986). The width parameter equation is used for cohesionless soils but it neglects the impact of different sand soil densities. Therefore, the differences between surface displacement profiles obtained by the FEA and those obtained by the SDE may be due to the value of the shear strength and stress parameters for the soil media around tunnel system. Figs. 10 to 13 show the comparison between the results obtained by both the FEA and the SDE. The surface settlements due to tunnelling are calculated by the SDE with different (a) and (n) parameters.

It is also observed that the FEA takes into account the effects of volume losses. However, the surface displacement equation does not consider the impact of the volume loss. The volume loss is an important parameter effect on the performance of the tunnel system. An increase of volume loss from 1.5% to 4.5% leads to increases the estimated surface settlements due to tunnelling by up to 60%. The smaller the volume loss due to tunnelling the smaller the calculated surface settlement.

In the case of loose sand, the surface displacement profiles obtained by the FEA are examined with those obtained by the SDE. The surface displacements calculated by the SDE are very close to those calculated by the FEA as the (a) parameter is ranged from 0.92 to 0.95 at (n) parameter found to be 1.0.

In the case of medium sand, the surface displacement profiles obtained by the FEA are examined with those obtained by the SDE. The surface displacements calculated by the SDE are very close to those calculated by the FEA as the (a) parameter is ranged from 0.89 to 0.92 at (n) parameter found to be 1.0.

In the case of dense sand, the surface displacement profiles obtained by the FEA are examined with those obtained by the SDE. The surface displacements calculated by the SDE are very close to those calculated by the FEA as the (a) parameter is ranged from 0.86 to 0.89 at (n) parameter found to be 1.0.

In the case of very dense sand, the surface displacement profiles obtained by the FEA are examined with those obtained by the SDE. The surface displacements calculated by the SDE are very close to those calculated by the FEA as the (a) parameter is ranged from 0.82 to 0.86 at (n) parameter found to be 1.0.

Therefore, the finite element analysis gives a better estimation of surface settlement as demonstrated with the comparison between the calculated and the measured surface settlements based on the case study.

At inflection point shown in Fig. 9 due to tunnelling, the results show that the surface displacements calculated by the SDE differ from those obtained by the FEA by up to 20% based

Table 4 The (a) parameter used at the (i) parameter equation at different sand soil densities

S/N	Sand soil condition	n-parameter	a-parameter
1	loose sand	1	0.92- 0.94
2	medium sand	1	0.9- 0.92
3	dense sand	1	0.88- 0.9
4	very dense sand	1	0.86- 0.88

on different values of (a) parameters. These differences between readings may lead to damage surrounding buildings due to surface and subsurface ground subsidence. Based on the 2-D FEA, the new (a) parameter captured in this study leads to minimize the reading discrepancy obtained by both the SDE and the FEA. Figs. 10 to 13 also show that the (n) parameter used at the (i) parameter does not give a big difference in the surface settlement. However, the (n) parameter used at the (i) width parameter is found to be constant value ($n = 1.0$). Based on the (n) parameter to be equal 1, the width parameter equation (i) is used to capture the new (a) parameter at different sand soil densities based on the FEA. Therefore, this study captures the value of the (a) parameter for different sand soil types as summarized in Table 4.

10. Conclusions

From the foregoing study, it is clear that the 2-D nonlinear FEA can be used to analysis the tunnel performance. The following conclusions can be drawn regarding the performance of the tunnel under the effects of different sand soil densities.

- The 2-D nonlinear finite element analysis is applicable to analyze and predict detailed displacements calculated by the SDE are very close to those obtained from the FEA as th performance of tunnel systems.
- The results obtained from the 2-D finite element analysis have a good agreement with the field data.
- The (n) parameter used in the (i) width parameter does not give a big difference in the surface settlement calculated by the SDE.
- The (a) parameter used in the (i) width parameter has significant effect on the surface settlement calculated by SDE.
- In the case of loose sand, the surface e (a) parameter varies from 0.92 to 0.95 and the (n) parameter is found to be 1.0.
- In the case of medium sand, the surface displacements calculated by the SDE are very close to those obtained from the FEA as the (a) parameter varies from 0.89 to 0.92 and the (n) parameter is found to be 1.0.
- In the case of dense sand, the surface displacements calculated by the SDE are very close to those obtained from the FEA as the (a) parameter varies from 0.86 to 0.89 and the (n) parameter is found to be 1.0.
- In the case of very dense sand the surface displacements calculated by the SDE are very close to those obtained from the FEA as the (a) parameter varies from 0.82 to 0.86 and the (n) parameter is found to be 1.0.

Acknowledgments

The author acknowledges the National Authority for Tunnels (NAT) and the Egyptian Tunnelling Society for the technical support.

References

- Abu-Farsakh, M.Y. and Tumay, M.T. (1999), "Finite element analysis of ground response due to tunnel excavation in soils", *Proceeding of the International Journal for Numerical and Analytical Methods in Geomechanics*, Vol. 23, pp. 524-539.
- Abu-Krishna, A. (2001), "Settlement control of CWO Sewer tunnel during boring El-Azhar road tunnels in Cairo", *Proceeding of the International World to Congress Milano*, Italy, pp. 3-9.
- Attwell, P.B., Yeates, J. and Selby, A.R. (1986), *Soil Movement Induced by Tunnelling and Their Effects on Pipelines and Structures*, Blackie and Son Ltd., Chapman and Hall, USA.
- Bicel, J.O. and Kuesel, T.R. (1982), *Tunnel Engineering Hand Book*, Van Nostrand Reinhold Company, New York, USA.
- Cavalaro, S.H.P., Blom, C.B.M., Walraven, J.C. and Aguado, A. (2011), "Structure analysis of control deficiencies in segmented lining", *Tunnel. Undergr. Space Tech.*, **26**(6), 115-127.
- Cehade, F.H. and Shahrour, I. (2008), "Numerical analysis of the interaction between twin-tunnels: Influence of the relative position and construction procedure", *Tunnel. Undergr. Space Tech.*, **23**(2), 210-224.
- Chen, W.F. and Mizuno, E. (1990), *Nonlinear Analysis in Soil Mechanics*, Elsevier Science Publishers, Netherlands.
- Darabi, A., Ahangari Kaveh, A., Noorzad, A. and Arab, A. (2012), "Subsidence estimation utilizing various approaches – A case study: Tehran No. 3 subway line", *Tunnel. Undergr. Space Tech.*, **31**, 117-127.
- Duncan, J.M., Byrne, P.M., Wong, K.S. and Mabry, P. (1980), "Strength, stress-strain, and bulk modulus parameters for finite element analysis of stresses and movements in soil masses", Report No. UCB/GT/80-01, University of California, Berkeley, CA, USA.
- El-Nahhass, F.M. (1986), "Spatial mode of ground subsidence above advancing shielded tunnels", *Proceeding of International Congress on Large underground Opening*, Firenze, Italy, Vol. 1, pp. 720-725.
- El-Nahhass, F.M. (1999), "Soft ground tunnelling in Egypt: Geotechnical challenges and expectations", *Tunnel. Undergr. Space Tech.*, **14**(3), 245-256.
- Elsayed, A.A. (2011), "Study of rock-lining interaction for circular tunnels using finite element analysis", *Jordan J. Civil Eng.*, **5**(1), 50-64.
- Garner, C. and Coffman, R. (2013), "Subway tunnel design using ground surface settlement profile to characterize an acceptable configuration", *Tunnel. Undergr. Space Tech.*, **35**, 219-226.
- Janbu, N. (1963), "Soil compressibility as determined by oedometer and triaxial tests", *European Conference on Soil Mechanics of Foundation Engineering*, Wiesbaden, Germany, Vol. 1, pp. 19-25.
- Jongpradist, P., Kaewsri, T., Sawatparnich, A., Suwansawat, S., Youwai, S., Kongkitkul, W. and Sunitsakul, J. (2013), "Development of tunnelling influence zones for adjacent pile foundations by numerical analysis", *Tunnel. Undergr. Space Tech.*, **34**, pp. 96-109.
- Liu, J.F., Qi, T.Y. and Wu, Z.R. (2012), "Analysis of ground movement due to metro tunnel station driven with enlarging shield tunnels under building and its parameter sensitivity analysis", *Tunnel. Undergr. Space Tech.*, **28**, 287-296.
- Mazek, S.A. (2004), "3-D elasto- plastic finite element analysis of crossing tunnels", *Proceeding of the 5th International Conference on Civil and Architecture Engineering (ICCAE)*, Military Technical College, Cairo, Egypt, November, pp. 364-377.
- Mazek, S.A. (2005), "Impact of grouting on an existing tunnel performance under passed by another tunnel", *Proceedings of the 11th International Colloquium on Structural and Geotechnical Engineering (ICSGE)*,

- Ain Shams University, Cairo, Egypt, May.
- Mazek, S.A. and El-Tehawy, E.M. (2008), "Impact of tunnelling running side-by-side to an existing tunnel on tunnel performance using non-linear analysis", *Proceedings of the 7th International Conference on Civil and Architecture Engineering (ICCAE)*, Cairo, Egypt, May.
- Mazek, S.A., Law, K.T. and Lau, D.T. (2004), "Numerical analysis of crossing tunnel performance", *Proceedings of the 5th International Conference on Civil and Architecture Engineering (ICCAE)*, Military Technical College, Cairo, Egypt, November, pp. 378-390.
- Mroueh, H. and Shahrour, I. (2008), "A simplified 3D model for tunnel construction using tunnel boring machines", *Tunnel. Undergr. Space Tech.*, **23**, 38-45.
- National Authority for Tunnels (NAT) (1993), Project document of the Greater Cairo metro tunnel (Line 2), Cairo, Egypt.
- National Authority for Tunnels (NAT) (1999), Project document of El-Azhar road tunnels, Cairo, Egypt.
- National Authority for Tunnels (NAT) (2010), Project document of the Greater Cairo metro tunnel (Line 3), Cairo, Egypt.
- Oettl, G., Stark, R.F. and Hofstetter, G.A. (1998), "Comparison of elastic-plastic soil models for 2-D FE analyses of tunnelling", *Comput. Geotech.*, **23**(1-2), pp. 19-38.
- Peck, R.B. and Schmidt, B. (1969), "Deep excavations and tunnelling in soft ground", *Proceedings of the 7th Conference on Soil Mechanics and Foundation Engineering*, Mexico City, Mexico, pp. 225-290.
- Valizadeh Kivi, A., Sadaghiani, M.H. and Ahmadi, M.M. (2012), "Numerical modeling of ground settlement control large span underground metro station in Tehran metro using central beam column (CBC)", *Tunnel. Undergr. Space Tech.*, **28**, 218-228.
- Vermeer, P.A. and Moller, S.C. (2008), "On numerical simulation of tunnel installation", *Tunnel. Undergr. Space Tech.*, **23**(4), 461-475.
- Wang, Y., Shi, J.W. and Ng, C.W.W. (2011), "Numerical modeling of tunnelling effect on buried pipelines", *Can. Geotech. J.*, **48**(7), 1125-1137.
- Wang, Z.C., Wong, R.C.K., Li, S.C. and Qiao, L.P. (2012), "Finite element analysis of long-term surface settlement above a shallow tunnel in soft ground", *Tunnel. Undergr. Space Tech.*, **30**, 85-92.
- Wong, K.S. and Duncan, J.M. (1974), "Hyperbolic stress-strain parameters for nonlinear finite element analyses of stresses and movements in soil masses", Report No. TE 74-3, University of California, Berkeley, California, USA.
- Zhang, Z., Huang, M. and Zhang, M. (2011), "Theoretical prediction of ground movements induced by tunnelling in multi-layered soils", *Tunnel. Undergr. Space Tech.*, **26**(2), 345-355.